Polish Journal of Microbiology
2021, Vol. 70, No 4, 447–459
https://doi.org/10.33073/pjm-2021-041

ORIGINAL PAPER

Chemical Components of Aqueous Extracts of *Melia azedarach* Fruits and Their Effects on The Transcriptome of *Staphylococcus aureus*

HONG PENG[1#], YING-SI WANG[1#], JIE WANG[2#], SU-JUAN LI[1], TING-LI SUN[1], TONG LIU[1, 2], QING-SHAN SHI[1, 2*], GANG ZHOU[1, 2*] and XIAO-BAO XIE[1, 2*]

[1] Guangdong Provincial Key Laboratory of Microbial Culture Collection and Application, State Key Laboratory of Applied Microbiology Southern China, Institute of Microbiology, Guangdong Academy of Sciences, Guangzhou, People's Republic of China
[2] College of Food Science, South China Agricultural University, Guangzhou, People's Republic of China

Submitted 20 June 2021, accepted 15 September 2021, published online 29 October 2021

Abstract

Staphylococcus aureus is the causative agent of numerous and varied clinical infections. Crude aqueous extracts of *Melia azedarach* fruits inhibit the planktonic growth and initial biofilm formation of *S. aureus* in a dose-dependent manner. Moreover, the biofilm topologies became sparse and decreased as the concentration of the aqueous extracts increased. RNA-Seq analyses revealed 532 differentially expressed genes (DEGs) after *S. aureus* exposure to 0.25 g/ml extracts; 319 of them were upregulated, and 213 were downregulated. The majority of DEGs were categorized into abundant sub-groups in the Gene Ontology (GO) and Kyoto Encyclopedia of Genes and Genomes (KEGG) pathways. Finally, untargeted UHPLC-MS/MS analyses of the aqueous extracts of *M. azedarach* fruits demonstrated a highly complex profile in positive and negative electrospray ionization modes. The extracts primarily consisted of lipids and lipid-like molecules, organic acids and their derivatives, phenylpropanoids, polyketides, organoheterocyclic compounds, and benzenoids annotated by abundant lipid maps and KEGG pathways. Overall, this study provides evidences that the aqueous extracts of *M. azedarach* fruits can control *S. aureus* infections and sought to understand the mode of action of these extracts on *S. aureus*.

Graphical abstrct

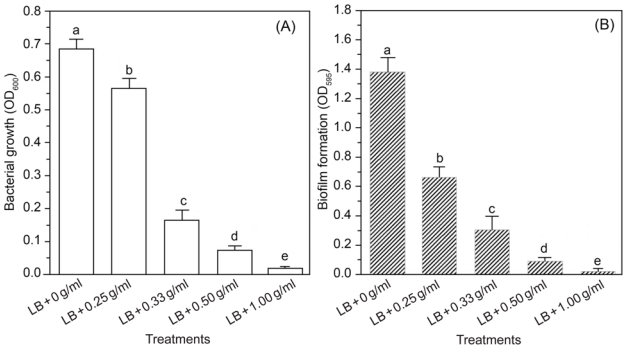

The planktonic growth (A) and biofilm formation (B) of *Staphylococcus aureus* can be inhibited by aqueous extracts of *Melia azedarach* fruits in a dose-dependent manner

K e y w o r d s: *Staphylococcus aureus*, *Melia azedarach* fruits, differentially expressed genes, biofilms, UHPLC-MS/MS

Introduction

Melia azedarach (chinaberry) tolerates a wide range of adverse environmental settings so that it is commonly found in tropical, subtropical, and warm temperate areas as an ornamental plant, shade tree, and a source of fuel (Khan et al. 2011). In the past decades, various components have been extracted from chinaberry leaves, bark, fruits, and roots with different approaches. The active ingredients exhibited antimicrobial

# Hong Peng, Ying-Si Wang and Jie Wang contributed equally to this study.

* Corresponding authors: Q.-S. Shi, Guangdong Provincial Key Laboratory of Microbial Culture Collection and Application, State Key Laboratory of Applied Microbiology Southern China, Institute of Microbiology, Guangdong Academy of Sciences, Guangzhou, People's Republic of China; College of Food Science, South China Agricultural University, Guangzhou, People's Republic of China; **e-mail: shiqingshan@hotmail.com**
G.Zhou, Guangdong Provincial Key Laboratory of Microbial Culture Collection and Application, State Key Laboratory of Applied Microbiology Southern China, Institute of Microbiology, Guangdong Academy of Sciences, Guangzhou, People's Republic of China; College of Food Science, South China Agricultural University, Guangzhou, People's Republic of China; **e-mail: zgbees@gdim.cn**
X.-B. Xie, Guangdong Provincial Key Laboratory of Microbial Culture Collection and Application, State Key Laboratory of Applied Microbiology Southern China, Institute of Microbiology, Guangdong Academy of Sciences, Guangzhou, People's Republic of China; College of Food Science, South China Agricultural University, Guangzhou, People's Republic of China; **e-mail: xiexb@gdim.cn**

activities, which might be affected by the solvents used in the extraction and the parts of this plant that the extracts were from (Khan et al. 2011; Zahoor et al. 2015). Chinaberry leaves, roots, and bark extracted with methanol, petrol, dichloromethane, and ethyl acetate exhibited a broad spectrum of antibacterial activity, but the dichloromethane fraction of the bark was the most effective (Khan et al. 2001). A methanol extract of chinaberry flowers demonstrated potential antibacterial effects on *Staphylococcus aureus* when evaluated with a rabbit skin infection model (Saleem et al. 2002).

The antibacterial activities of chinaberry leaves extract in aqueous or chloroform on two Gram-positive bacteria, *Bacillus subtilis* and *S. aureus*, and three Gram-negative bacteria, *Escherichia coli*, *Pseudomonas aeruginosa*, and *Klebsiella pneumoniae*, were assessed using the agar well diffusion method. The extracts exhibited a relatively higher zone of inhibition at 75 µl/ml than at concentrations of 25 and 50 µl/ml, and the aqueous extracts were more effective at inhibiting the bacteria than those extracted in chloroform at the specific concentrations tested. It suggests that the leaf extracts caused inhibition in a dose-dependent manner, and the solvents used in extraction also influenced the activities (Suresh et al. 2008).

However, another study found that the alcoholic extracts of chinaberry leaves were more potent than those extracted with methanol, petroleum ether, and water when tested against eight human pathogens, including *E. coli*, *P. aeruginosa*, *B. cereus*, *S. aureus*, *Fusarium oxisporum*, *Aspergillus niger*, *Rhizopus stolonifera,* and *Aspergillus flavus* (Sen and Batra 2012). Antibacterial activities of the crude methanolic extracts of chinaberry were measured using an agar well diffusion method, but *E. coli* was highly resistant to the extracts at all doses tested (Zulqarnain et al. 2015). It suggests that the antibacterial activity of crude extracts of chinaberry varies with the microorganisms' species.

In addition, the antibacterial spectrum of the same chinaberry extracts was affected by the solvents used in the extraction process. The antimicrobial, antioxidant, and cytotoxic activities of chinaberry bark extracted with various solvents were assayed. The results showed that the chloroform extract was active against both *Enterobacter aerogenes* and *Proteus mirabilis*, while both *n*-hexane and butanol were the most effective at inhibiting *E. aerogenes*. Simultaneously, aqueous and methanolic extracts were the most effective against *P. mirabilis*, and ethyl acetate was the most effective against *P. aeruginosa* (Zahoor et al. 2015).

Bacterial biofilms are complex, multi-species bacterial communities that are usually highly resistant to antimicrobial agents (Mah 2012; Zhou et al. 2015). However, chinaberry extracts have been shown to have strong antimicrobial effects against the microorganisms producing recalcitrant biofilm, including *Acinetobacter guillouiae*, *Alcaligenes faecalis*, *Bacillus pumilus*, *Bacillus safensis*, *Brevundimonas alba*, *Microbacterium lacticum*, *Staphylococcus equorum*, and *Staphylococcus saprophyticus*, which were isolated from dental plaques (Khalid et al. 2017).

In addition to their antibacterial activities, the bioactive phytochemicals were also isolated and identified from chinaberry extracts. The human pathogens *Enterococcus faecalis*, *E. coli*, *P. aeruginosa* and *Klebsiella oxytoca* were susceptible to extracts from chinaberry leaves, particularly the petroleum ether fraction that consists of secondary metabolites, such as alkaloids, terpenes/sterols, saponins, tannins and anthocyanins (Rojas Sierra et al. 2012). A variety of compounds have been found in the methanolic extracts from chinaberry, including propanedioic acid, butanedioic acid, diethyl ester, 2-pyrrolidinyl-methylamine, 2-piperidimethanamine, and trichloromethane (Al-Marzoqi et al. 2015). In addition, a substantial number of different ingredients were also isolated and identified from chinaberry by different research groups, which repeatedly demonstrated that the components of extracts varied with the extracted parts, solvents, and methodology.

Taken together, the antimicrobial activities and bioactive agents of extracts of chinaberry have been widely studied by different laboratories. However, the underlying modes of action of these extracts on bacteria remain elusive. Thus, in this study, we tried to extract components from chinaberry fruits using simple boiling water methods, and the differentially expressed genes (DEGs) were detected with RNA-Seq using *S. aureus* as a model strain. The results demonstrated that various growth and metabolism-related genes and pathways were affected by the aqueous extracts of chinaberry fruits. Moreover, lipids and lipid-like molecules, organic acids, and derivatives were relatively abundant in these extracts.

Experimental

Materials and Methods

Bacterial strains and chemicals. The bacterial strain *S. aureus* ATCC 6538 was purchased from the American Type Culture Collection (ATCC) and was cultivated in Luria Bertani (LB) medium that consisted of 5 g/l yeast extract (Oxoid, Hampshire, England), 10 g/l NaCl (Sigma-Aldrich, St. Louis, MO, USA) and 10 g/l peptone (Oxoid) without any antibiotics at 37°C in a shaking incubator. All the chemicals used in this study were of analytical grade and supplied by Sigma-Aldrich (St. Louis, MO, USA) unless indicated otherwise.

Extractions of chinaberry fruits with water. The chinaberry fruits purchased in Sichuan (China) were first washed with pure water to remove dust, dried to a constant weight at 65°C, and then crushed into powders using a grinder (Tianchuang Powder Technology Co., Ltd., Changsha, China). An aliquot of 100 g of the ground powders was weighed and dissolved in 1,000 ml of distilled water, sonicated with an ultrasound instrument (Anpu Experimental Technology Co, Ltd., Shanghai, China) for 30 min at room temperature, heated, and boiled for 30 min, and sonicated again for another 30 min. The samples were filtered with 200-mesh gauze to obtain the crude extracts. The filter residues were subsequently added to 500 ml of distilled water, boiled for another 30 min, filtered with 200-mesh gauze, and the extracts obtained were combined with the previous extracts and centrifuged at 13,000 rpm for 10 min. The supernatants were then transferred into a new plastic tube, filtered through a 400-mesh nylon filter using a gas-liquid diaphragm vacuum pump (Huankai Microbiology Technology Co. Ltd., Guangzhou, China), and the filtered samples were re-filtered through a 0.45-μm membrane using the same vacuum pump. Finally, the samples that had been filtered twice were placed in a rotary evaporator (Ailang Instrument Co. Ltd., Shanghai, China) with a vacuum degree of –0.1 ~ –0.08 MPa to concentrate the liquid to 100 ml under reduced pressure to ensure that the final concentration of the bioactive reagents was approximately 1.00 g/ml. After sterilization at 121°C for 20 min, the concentrated extracts were stored in a refrigerator at 4°C for future use.

Semi-quantitative measurements of *S. aureus* biofilms. The biofilm biomass formed by *S. aureus* was measured using a crystal violet staining method in flat-bottomed polystyrene microtiter plates (Corning Inc., Corning, NY, USA), as previously described with minor modifications (Stepanović et al. 2000; Zhou et al. 2019). Briefly, each well of one column of a 96-well microtiter plate was inoculated with 150 μl of *S. aureus* suspensions with an optical density (OD_{600}) of approximately 0.05 and 50 μl of aqueous extracts of chinaberry fruits to final concentrations of 0, 0.25, 0.33, 0.50, and 1.00 g/ml. Moreover, the negative controls contained only LB medium. The inoculated plates were then placed in a static incubator with a constant temperature at 37°C and cultured for 48 h. Before staining, the OD_{600} of planktonic cells was detected with a Multiskan GO plate reader (Thermo Fisher Scientific, Waltham, MA, USA). Next, the plates were gently washed three times with sterile water to remove all the planktonic cells. The biofilms formed on the inner wall of the plates were finally stained with 250 μl of crystal violet (0.1%, w/v; Shanghai Chemical Reagents Co. Ltd., Shanghai, China) for at least 30 min at room temperature. After removing the crystal violet, the stained biofilms in each well were finally dissolved in 260 μl of 95% ethanol (v/v; Shanghai Chemical Reagents Co. Ltd.), and the OD_{590} of each well was determined using the same Multiskan GO reader (Thermo Fisher Scientific). All the experiments were conducted with eight replicates and repeated at least three times on different days.

Confocal laser scanning microscopy (CLSM) observation of biofilm topographies. The biofilms of *S. aureus* that had formed on pre-sterilized glass cover slides were observed by CLSM as previously described with minor modifications (Shukla and Rao 2013; Zhou et al. 2013). Briefly, the wells of a 24-well polystyrene microtiter plate with glass coverslips inside were inoculated with 2 ml aliquots of *S. aureus* suspensions (final $OD_{600} = 0.05$), and different concentrations of water extracts of chinaberry fruits (final concentrations 0, 0.25, 0.33, 0.50, and 1.00 g/ml). The microtiter plates were then transferred to an incubator and incubated at static conditions at 37°C for 48 h. To assay the biomass and observe the topographies of the attached *S. aureus* biofilms, 5 μM of SYTO9 fluorescent dye (Invitrogen, Carlsbad, CA, USA) was used to dye the slips for 20 min in the dark, as previously reported (GrayMerod et al. 2005). Finally, the stained biofilms were visualized and photographed using a Zeiss LSM 710 (Jena, Germany), and the live bacteria encased in the biofilms were dyed fluorescent green. The CLSM images obtained under different conditions were analyzed in more detail using COMSAT 2.1 software to evaluate the biomass, maximum, and average height of the biofilms formed (Heydorn et al. 2000).

Transcriptomic sequencing (RNA-Seq) and data analyses. *S. aureus* was cultured statically in 96-well microtiter plates in the presence of 0.25 g/ml aqueous extracts of chinaberry fruits at 37°C. After 2 days of cultivation, the cultured planktonic cells of *S. aureus* were harvested from wells, the pellets were collected by centrifugation, and sent to the Guangzhou Meige Biotechnology Company (Guangzhou, China) for RNA extraction and RNA-Seq library preparation. The chinaberry fruits cultured without any water extracts were the control samples, and were simultaneously sent to the sequencing company. After cluster generation, the prepared RNA-Seq library was then sequenced on an Illumina NovaSeq platform (San Diego, CA, USA), and the paired-end reads of 150 bp were generated. Moreover, the clean data were acquired by removing low-quality reads and the reads that contained adapter and ploy-N from raw data. Differential expression analyses of the two conditions/groups were calculated using the DESeq R package (1.18.0). Moreover, the approach of Benjamini and Hochberg was used to adjust the resulting *p*-values to control the false discovery rate. DEGs were assigned with an adjusted value of $p < 0.05$ and $|\text{fold-change}| > 1.5$. Gene Ontology (GO)

enrichment analyses of the DEGs were processed using the GOseq R package, in which the gene length bias was synchronously corrected. Moreover, GO terms with corrected *p*-values less than 0.05 were considered to be significantly enriched by DEGs. In addition, the KOBAS software was utilized to test the statistical enrichment of DEGs in KEGG pathways (https://www.kegg.jp/kegg/pathway.html). In addition, the clean transcriptomic sequencing data were deposited in the NCBI Sequence Read Archive (SRA) under BioProject ID PRJNA723959.

Chemical composition of the aqueous extracts from chinaberry fruits. The chemical composition of aqueous extracts from chinaberry fruits was analyzed as previously described (Liu et al. 2020; Wright Muelas et al. 2020; Grabowska et al. 2021). A Vanquish UHPLC system (Thermo Fisher Scientific) equipped with an Orbitrap Q Exactive series mass spectrometer (Thermo Fisher Scientific) was utilized to analyze the chemicals from the LC-MS/MS chinaberry fruit extracts. The treated and filtered samples were transferred into a Hypersil Gold column (100 × 2.1 mm, 1.9 μm; Thermo Fisher Scientific) operating at a column temperature of 50°C. The samples were eluted at 0.4 ml/min flow rate over 15 min with 0.1% formic acid in water (solvent A) and 0.1% formic acid in methanol (solvent B). Moreover, 5 mM ammonium acetate at pH 9.0 (solvent A) and methanol (solvent B) were used as eluents in the negative polarity mode. The solvent gradient was performed as follows: 2% B, 1.5 min; 2–100% B, 12.0 min; 100% B, 14.0 min; 100–2% B, 14.1 min; and 2% B, 17 min. The Q Exactive series mass spectrometer (Thermo Fisher Scientific) was operated in a positive or negative polarity mode with a capillary temperature of 320°C, a spray voltage of 3.2 kV, an auxiliary gas flow rate 10 arb, and a sheath gas flow rate of 35 arb. The raw data files obtained by UHPLC-MS/MS were then processed with Compound Discoverer CD3.1 software (Thermo Fisher Scientific) to align the peaks and picks and quantify each metabolite. The main parameters in the analyses were set as follows: retention time tolerance, 0.2 min; signal intensity tolerance, 30%; actual mass tolerance, 5 ppm; minimum intensity, 100,000 and signal/noise ratio, 3; respectively. Subsequently, the acquired peak intensities were then normalized to the total spectral intensity. The acquired normalized data were continuously used to predict the molecular formula based on the molecular ion peaks, additive ions, and fragment ions. Finally, the peaks were processed to match the mzVault 2.1, mzCloud (https://www.mzcloud.org/), and MassList databases to obtain accurate and relative quantitative results. Statistical analyses in this section were performed with the statistical software R (version: R-3.4.3), Python (version: 2.7.6), and CentOS (CentOS release 6.6). Furthermore, the HMDB (http://www.hmdb.ca/), LipidMaps (http://www.lipidmaps.org/), and Kyoto Encyclopedia of Genes and Genomes (KEGG) databases (http://www.genome.jp/kegg/) were utilized to conduct the annotation of all metabolites identified.

Statistical analysis. All the data obtained were expressed as the mean ± standard deviation (SD) and were then subjected to a one-way analysis of variance (ANOVA) followed by comparing multiple treatment levels with the control using the Fisher's LSD test. Moreover, when p-value < 0.05 was considered as significant. The statistical analyses were calculated using the data processing system (DPS) software (Tang and Feng 2007).

Results

Aqueous extracts of chinaberry fruits exhibit inhibitory effects on both planktonic growth and biofilm formation of *S. aureus*. In this study, the active components were extracted from chinaberry fruits using a simple water boiling method. The aqueous extracts were then used to test their effects on planktonic growth and the initial *S. aureus* biofilm formation in a static condition in 96-well microtiter plates. As expected, the planktonic growth of *S. aureus* was inhibited by the aqueous extracts of chinaberry fruits in a dose-dependent manner (Fig. 1A). In the presence of 0.25, 0.33, 0.50, and 1.00 g/ml aqueous extracts, the planktonic growth of *S. aureus* was repressed by approximately 17.63%, 76.05%, 89.32%, and 97.27%, respectively, compared with the controls (Fig. 1A). Furthermore, the biofilm formation of *S. aureus* treated with the same concentrations of aqueous extracts of chinaberry fruits was assayed with the crystal violet staining method. The results demonstrated that the aqueous extracts also inhibited the biofilms of *S. aureus* in a dose-dependent manner (Fig. 1B), which is like the efficiencies of the inhibition of planktonic growth. When treated with 0.25, 0.33, 0.50, and 1.00 g/ml aqueous extracts, the biofilm formation of *S. aureus* was repressed by approximately 51.68%, 77.83%, 93.22%, and 98.30%, respectively, compared with the controls (Fig. 1B). These results revealed that aqueous extracts of chinaberry fruits can inhibit not only planktonic growth but also the *S. aureus* biofilm formation in a dose-dependent manner.

Biofilm topographies of *S. aureus* can be influenced by the aqueous extracts of chinaberry fruits. As shown in Fig. 1B, since the initial biofilm of *S. aureus* formed on a polystyrene surface can be influenced by the aqueous extracts of chinaberry fruits, we sought to determine whether the biofilm topographies of this strain built on a glass surface could be affected by these extracts. Therefore, the initial *S. aureus* biofilm

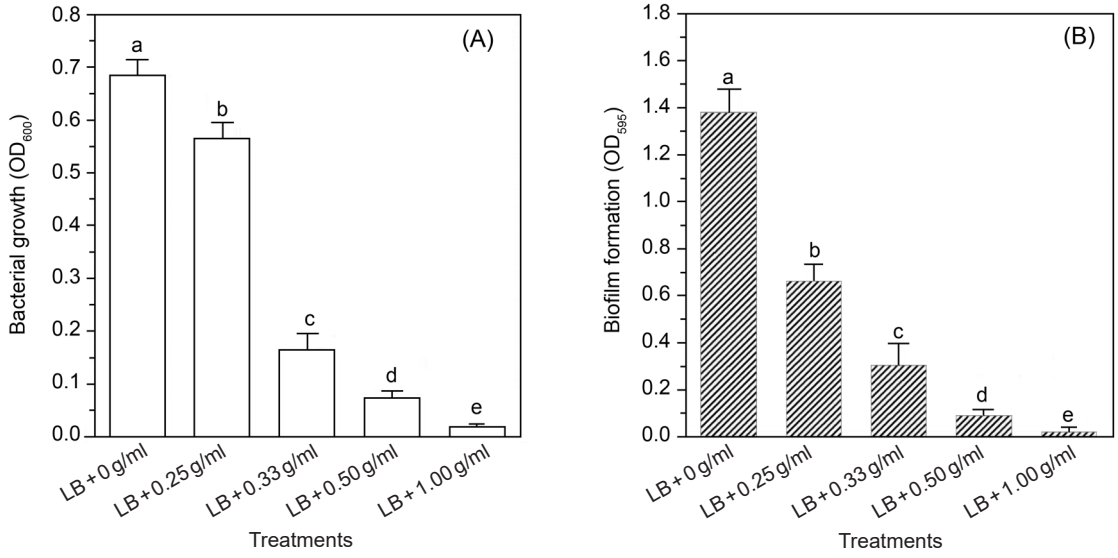

Fig. 1. Effect of aqueous extracts of *Melia azedarach* fruits on planktonic growth (A) and biofilm formation (B) of *Staphylococcus aureus* ATCC 6538. *S. aureus* ATCC 6538 was cultured on LB media supplemented with different concentrations of aqueous extracts of chinaberry fruits at 37°C for 48 h. The *S. aureus* planktonic cells and biofilms stained with crystal violet were measured at OD_{600} and OD_{590}, respectively, using a Multiskan GO plate reader.

was first allowed to be formed on glass cover slips, and then stained with the fluorescent dye SYTO9, and finally observed under CLSM. The results demonstrated that when cultured for 2 days, a typical *S. aureus* biofilm could be formed on the surface of the glass slips (Fig. 2A). However, the biofilms on these slips decreased and became sparse with the increasing concentrations of the aqueous extracts (Fig. 2B-2E). Furthermore, the biofilms-related parameters were also calculated using the COMSTAT based on the images obtained from CLSM. The results showed that the average thickness and total biomass, with the exception of maximum thickness, of

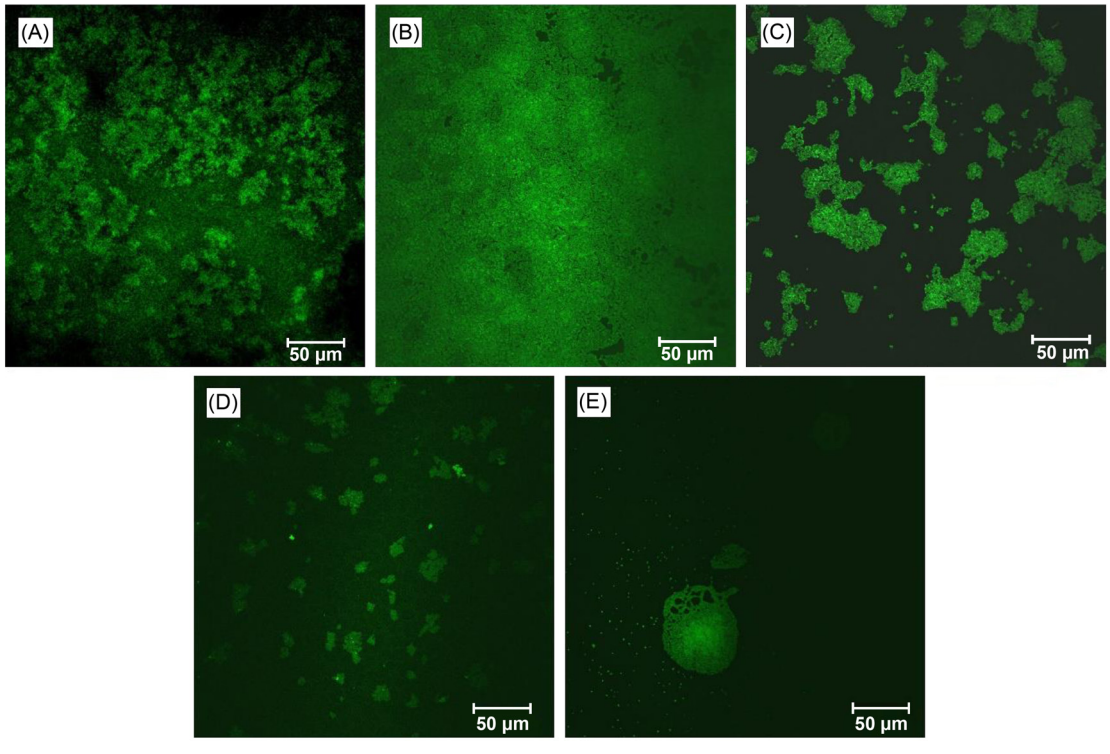

Fig. 2. Representative CLSM images of *Staphylococcus aureus* ATCC 6538 biofilms grown in the presence of different concentrations of aqueous extracts of *Melia azedarach* fruits and stained with SYTO9. The biofilms were cultivated on the surface of glass coverslips for 48 h at 37°C. The constructed biofilms were stained with the fluorescent dye SYTO9 and then observed under a Zeiss LSM 710 CLSM. Scale bar = 50 μm. CLSM, confocal laser scanning microscopy.

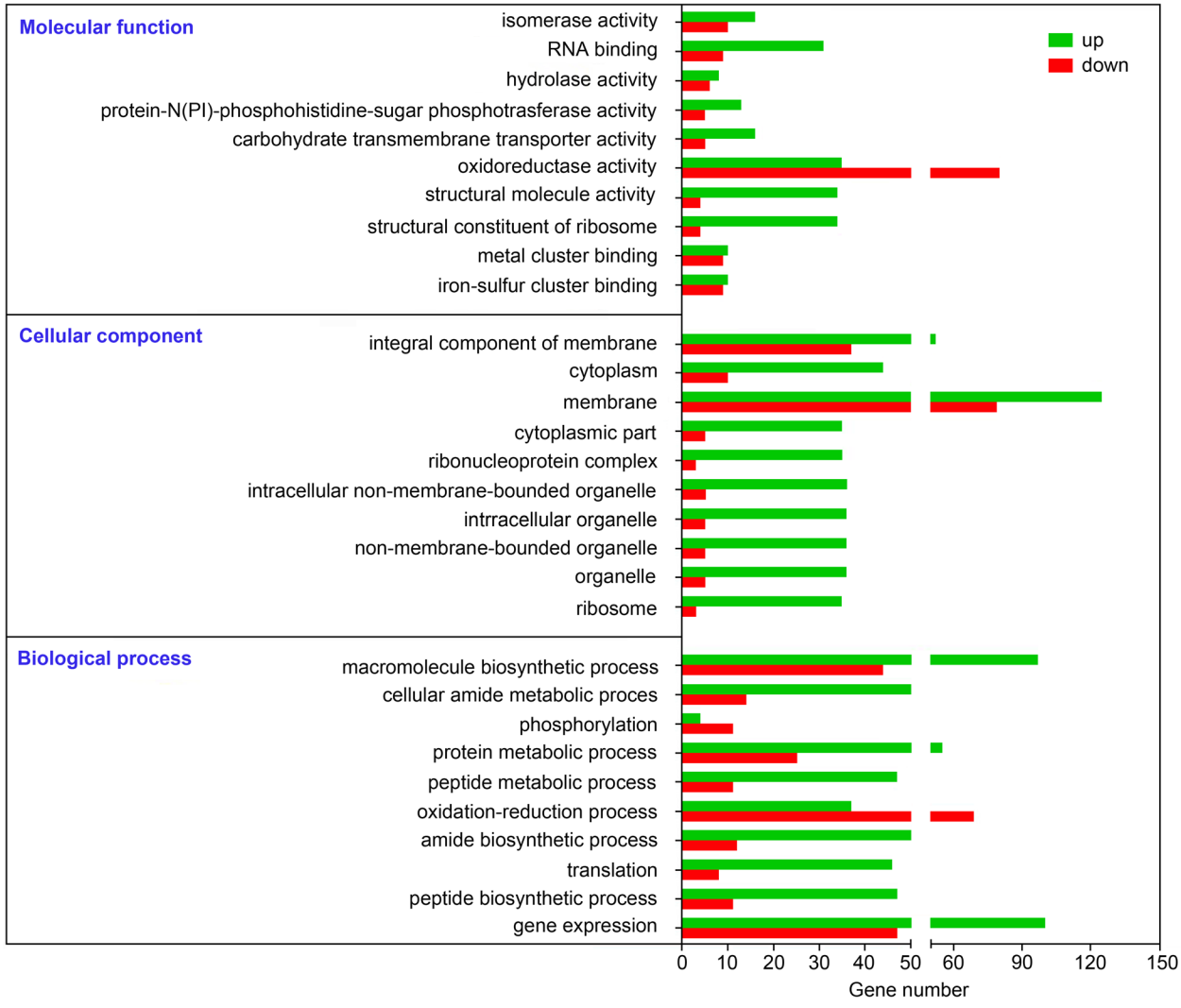

Fig. 3. Histogram depiction of enriched Gene Ontology classification of the DEGs of *Staphylococcus aureus* ATCC 6538 treated with 0.25 g/ml aqueous extracts of *Melia azedarach* fruits. The results were categorized into three main categories of biological process, molecular function, and cellular component. The x-axis indicates the gene numbers in each subcategory. The top 10 subcategories in each main category are shown here.

the formed biofilms that formed when cultured without aqueous extracts treatments were always higher than those harvested in the presence of various concentrations of aqueous extracts (Table I).

RNA-Seq results and DEGs. Since both bacterial growth and the initial biofilm formation of S. aureus could be inhibited by aqueous extracts of chinaberry fruits, our next goal was to elucidate the underlying modes of action of the aqueous extracts on *S. aureus* cells. Therefore, the samples of *S. aureus* planktonic cells treated with or without 0.25 g/ml aqueous extracts were harvested and subjected to RNA-Seq to acquire their transcriptome sequence data using an Illumina NovaSeq platform. The sequencing results identified 15,306,690; 16,228,122; 14,710,464; 15,424,438; 15,052,636; and 14,875,448 clean reads for the controls and treatments with three replicates, respectively. Moreover, the DEGs between controls and treatments were also analyzed with the DESeq R package (1.18.0). A total of 532 DEGs, of which 319 were activated, and 213 were inhibited, were identified when *S. aureus* planktonic cells were treated with 0.25 g/ml aqueous extracts of chinaberry fruits based on the following criteria identified: DESeq2 $p_{adj} < 0.05$ and $|\log2FoldChange| > 1.5$.

Various GO and KEGG pathways can be affected by the aqueous extracts of chinaberry fruits. In addition, GO analyses were also conducted to classify functions of the DEGs found in the RNA-Seq experiments. Based on the sequence homology, the DEGs were categorized into three classes that included biological process, cellular component, and molecular function, which have been shown as the first ten subgroups in each category (Fig. 3). Gene expression, membrane, and oxidoreductase activity were the largest subgroups enriched for the downregulated DEGs in biological

Table I
Quantification of biofilm topologies in the presence of different concentrations of aqueous extracts of *Melia azedarach* fruits.

Parameters	Control	0.25 g/ml	0.33 g/ml	0.50 g/ml	1.00 g/ml
Maximum thickness (μm)	10 ± 0.00^{a}	10 ± 0.00^{a}	10 ± 0.00^{a}	10 ± 0.00^{a}	10 ± 0.00^{a}
Average thickness (μm)	7.75 ± 0.10^{a}	6.68 ± 0.36^{b}	3.37 ± 0.17^{c}	2.11 ± 0.19^{d}	1.11 ± 0.03^{e}
Total biomass ($\mu m^3/\mu m^2$)	9.81 ± 1.78^{a}	6.97 ± 0.08^{b}	2.98 ± 0.25^{c}	1.40 ± 0.24^{cd}	0.22 ± 0.02^{d}

Different letters marked in the same row represent the significant differences among different treatments ($p < 0.05$)

process, cellular component, and molecular function, respectively (Fig. 3). Moreover, the oxidation-reduction process, membrane, and oxidoreductase activity were the most significant subgroups enriched for the up-regulated DEGs in biological process, cellular component, and molecular function, respectively (Fig. 3).

To further elucidate these DEGs' functions and explore the enriched metabolic or signal transduction pathways, the DEGs were also mapped to the terms from the KEGG pathway database (Fig. 4). Among the top 20 enriched KEGG pathways, the DEGs were significantly enriched for ribosome (KEGG pathway ID:

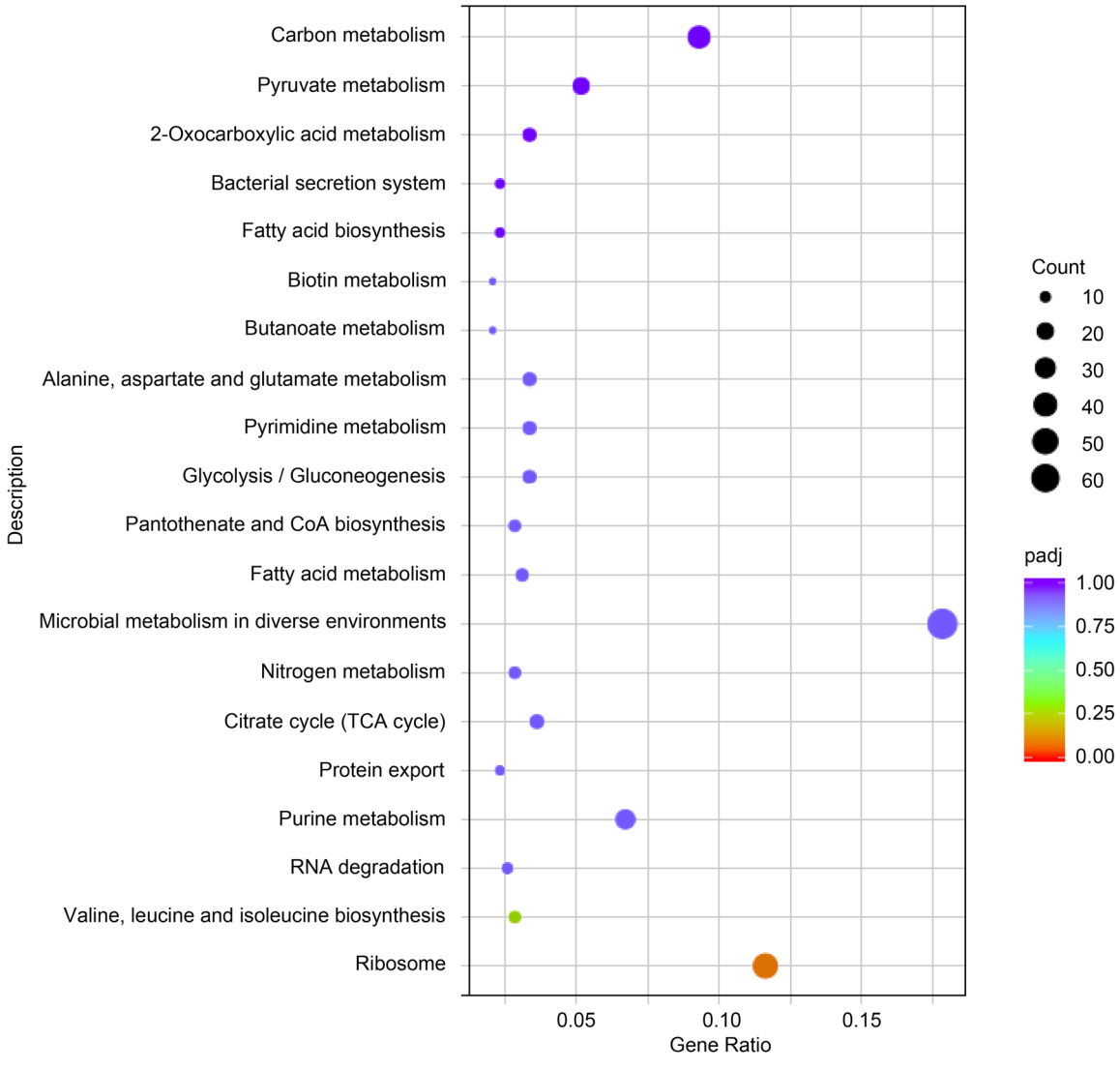

Fig. 4. Functional analysis of DEGs of *Staphylococcus aureus* ATCC 6538 treated with 0.25 g/ml aqueous extracts of *Melia azedarach* fruits based on the KEGG pathway. Among the top 20 pathways, the first two pathways, the ribosome (pae03010) and valine, leucine, and isoleucine biosynthesis (pae00290), were significantly enriched ($p_{adj} < 0.05$). The right y-axis represents the KEGG pathway. The x-axis exhibits the enrichment factor, which denotes the ratio of the DEG numbers to the annotated gene numbers enriched in a specific pathway. DEG, differentially expressed genes; KEGG, Kyoto Encyclopedia of Genes and Genomes.

Table II
Identification results of the top 25 metabolites from aqueous extracts of *Melia azedarach* fruits in a positive mode.

No.	Compound_ID	Name	Formula	Molecular Weight	Retention Time (min)
1	Com_2_pos	D-Pyrrolidine-2-Carboxylic acid	$C_5H_9NO_2$	115.0634	1.382
2	Com_3_pos	DL-Arginine	$C_6H_{14}N_4O_2$	174.1115	1.425
3	Com_6_pos	Choline	$C_5H_{13}NO$	103.0999	1.275
4	Com_49_pos	L-Glutamic acid	$C_5H_9NO_4$	147.0529	1.434
5	Com_28_pos	Nicotinic acid	$C_6H_5NO_2$	123.0321	1.773
6	Com_44_pos	Perillartine	$C_{10}H_{15}NO$	165.1152	7.342
7	Com_30_pos	6-Hydroxynicotinic acid	$C_6H_5NO_3$	139.0268	1.988
8	Com_59_pos	Maltol	$C_6H_6O_3$	126.0318	5.271
9	Com_21_pos	Isoamylamine	$C_5H_{13}N$	87.10517	4.875
10	Com_75_pos	5-oxoproline	$C_5H_7NO_3$	129.0426	1.45
11	Com_71_pos	Ethyl 4-amino-2-(methylsulfanyl)-1,3-thiazole--5-carboxylate	$C_7H_{10}N_2O_2S_2$	218.019	1.265
12	Com_77_pos	DL-Tryptophan	$C_{11}H_{12}N_2O_2$	204.0897	6.801
13	Com_98_pos	Ecgonine methyl ester	$C_{10}H_{17}NO_3$	199.1206	8.349
14	Com_103_pos	Scopoletin	$C_{10}H_8O_4$	192.0421	8.708
15	Com_105_pos	Gamma-Aminobutyric acid	$C_4H_9NO_2$	103.0637	1.292
16	Com_85_pos	Kinetin	$C_{10}H_9N_5O$	237.0635	2.048
17	Com_104_pos	N-Acetyl-DL-serine	$C_5H_9NO_4$	147.0529	1.284
18	Com_116_pos	Pipecolinic acid	$C_6H_{11}NO_2$	129.079	1.734
19	Com_119_pos	2-Methylenesuccinic acid	$C_5H_6O_4$	130.0263	1.284
20	Com_168_pos	2-Picolinic acid	$C_6H_5NO_2$	123.0321	1.523
21	Com_165_pos	6-O-(2-Methylbutanoyl)-α-D-glucopyranosyl α-D-glucopyranoside	$C_{17}H_{30}O_{12}$	443.1997	8.133
22	Com_135_pos	(+/-)12(13)-DiHOME	$C_{18}H_{34}O_4$	296.2345	14.142
23	Com_171_pos	Corylifol A	$C_{25}H_{26}O_4$	390.1823	10.9
24	Com_78_pos	Oleoyl ethylamide	$C_{20}H_{39}NO$	309.3025	15.542
25	Com_114_pos	Cytidine	$C_9H_{13}N_3O_5$	243.0893	8.013

pae03010) and valine, leucine, and isoleucine biosynthesis (pae00290).

Chemical components of the aqueous extracts of chinaberry fruits. Since *S. aureus* planktonic growth, biofilm formation, and the related GO and KEGG pathways could be influenced by the aqueous extracts of chinaberry fruits, we sought to determine the chemical components composed of these extracts. Thus, the chemical compositions of the aqueous extracts were characterized using a UHPLC-MS/MS-based non-targeted metabolomics approach to explain which active factors played roles in these biological processes. The results demonstrated that 681 and 339 metabolites were successfully identified under positive and negative ion modes, respectively. The basic characteristics of the top 25 metabolites in both the positive and negative ion modes are shown in Tables II and III, respectively. The detailed information, including the total ion intensity of the metabolites identified in chinaberry fruits' aqueous extracts, is shown in supplementary Excel files S1 and S2.

Functional annotation of the metabolites from aqueous extracts of chinaberry fruits. Three databases of HMDB, lipid maps, and KEGG pathways were used to annotate the functions of the metabolites from the aqueous extracts of chinaberry fruits. The annotation results demonstrated that a total of 242 and 148 metabolites under positive and negative ion modes were classified into 11 and 9 HMDB groups, respectively (Fig. 5). Among all the metabolites, 8.08% and 15.04% of the positive and negative ion modes referred to lipids and lipid-like molecules, respectively, following by organic acids and derivatives (6.46% and 8.26%, respectively), phenylpropanoids and polyketides (5.58% and 5.31%, respectively), organoheterocyclic compounds (5.43% and 4.72%, respectively), and benzenoids (3.52% and 3.83%, respectively; Fig. 5).

Furthermore, based on the classification notes of LIPID MAP, fatty acyls, polyketides, prenol lipids, and sterol lipids were found in both the positive and negative ion modes (Fig. 6). However, there are different numbers

Table III
Identification results of the top 25 metabolites from aqueous extracts of *Melia azedarach* fruits in a negative mode.

No.	Compound_ID	Name	Formula	Molecular Weight	Retention Time (min)
1	Com_2_neg	D-Saccharic acid	$C_6H_{10}O_8$	210.0372	1.174
2	Com_6_neg	Palmitic acid	$C_{16}H_{32}O_2$	256.2397	14.6
3	Com_4_neg	Citric acid	$C_6H_8O_7$	192.0267	1.214
4	Com_11_neg	N-Acetylneuraminic acid	$C_{11}H_{19}NO_9$	309.1055	1.296
5	Com_17_neg	Elaidic acid	$C_{18}H_{34}O_2$	282.2553	14.704
6	Com_15_neg	Sucrose	$C_{12}H_{22}O_{11}$	402.137	1.39
7	Com_22_neg	D-(−)-Lyxose	$C_5H_{10}O_5$	150.0526	1.268
8	Com_21_neg	Gluconic acid	$C_6H_{12}O_7$	196.058	1.256
9	Com_29_neg	DL-Malic acid	$C_4H_6O_5$	134.0214	1.186
10	Com_23_neg	4-Oxoproline	$C_5H_7NO_3$	83.03709	1.293
11	Com_31_neg	Pyruvic acid	$C_3H_4O_3$	88.01595	1.186
12	Com_25_neg	D-(−)-Fructose	$C_6H_{12}O_6$	180.0632	1.307
13	Com_48_neg	Glutaconic acid	$C_5H_6O_4$	130.0265	1.172
14	Com_56_neg	2-Furoic acid	$C_5H_4O_3$	112.016	1.155
15	Com_47_neg	Toosendanin	$C_{30}H_{38}O_{11}$	574.2414	11.083
16	Com_57_neg	α-Eleostearic acid	$C_{18}H_{30}O_2$	278.2241	14.157
17	Com_50_neg	α-Lactose	$C_{12}H_{22}O_{11}$	388.1213	1.373
18	Com_71_neg	Nomilin	$C_{28}H_{34}O_9$	514.2193	10.413
19	Com_54_neg	4-Acetamidobutanoic acid	$C_6H_{11}NO_3$	145.0739	1.439
20	Com_59_neg	D-(+)-Glucose	$C_6H_{12}O_6$	180.0632	1.484
21	Com_70_neg	6-Sialyllactose	$C_{23}H_{39}NO_{19}$	633.2127	1.319
22	Com_78_neg	Purine	$C_5H_4N_4$	120.0422	1.274
23	Com_77_neg	2-C-methyl D-erythritol 4-phosphate	$C_5H_{13}O_7P$	216.0399	1.27
24	Com_72_neg	Azelaic acid	$C_9H_{16}O_4$	188.1047	5.304
25	Com_81_neg	16-Hydroxyhexadecanoic acid	$C_{16}H_{32}O_3$	254.2242	14.26

of metabolites that are members of different groups from the positive and negative ion modes (Fig. 6).

In addition, the three main KEGG pathways of metabolism, genetic information processing, and environmental information processing were enriched for approximately 184 and 137 metabolites in the positive and negative ion modes, respectively (Fig. 7). In a positive mode, most metabolites take part in global and overview maps, biosynthesis of other secondary metabolites, and amino acid metabolism (Fig. 7). In contrast, in the negative mode, the pathways of global and overview maps, amino acid metabolism, and carbohydrate metabolism occupy most of the metabolites (Fig. 7).

Discussion

S. aureus is frequently found in the respiratory tract, human nose, and on the skin, so that it has been regarded as the most common cause of nosocomial infections (Archer 1998). However, it has been reported that the growth of *S. aureus* could be inhibited by the extracts of chinaberry leaves, barks, fruits, flowers, essential oils, and seeds (Kaneria et al. 2009; Liu et al. 2010; Kharkwal et al. 2015; Zulqarnain et al. 2015; Hadadi et al. 2020). Moreover, ordinary water was used as a solvent to extract active physiochemical ingredients from chinaberry. The antibacterial activity of chinaberry leaves was evaluated using an agar well diffusion method by measuring the inhibitory diameter of bacterial growth zones with 25, 50, and 75 µl of aqueous and solvent leaf extracts. The results indicated that the growth of *S. aureus* was inhibited by phytochemical compounds of aqueous extracts of chinaberry leaves, which is better than that extracted by chloroform in the three concentrations tested (Suresh et al. 2008).

In this study, we found that the crude aqueous extracts of chinaberry fruits inhibited *S. aureus* planktonic growth in a dose-dependent manner (Fig. 1A), although only water was used to extract the bioactive agents from the chinaberry fruits. Similar assays were also conducted by Sen and Batra (2012). However, they found that the antimicrobial activity of the aqueous extracts of chinaberry leaves to *S. aureus* exhibited

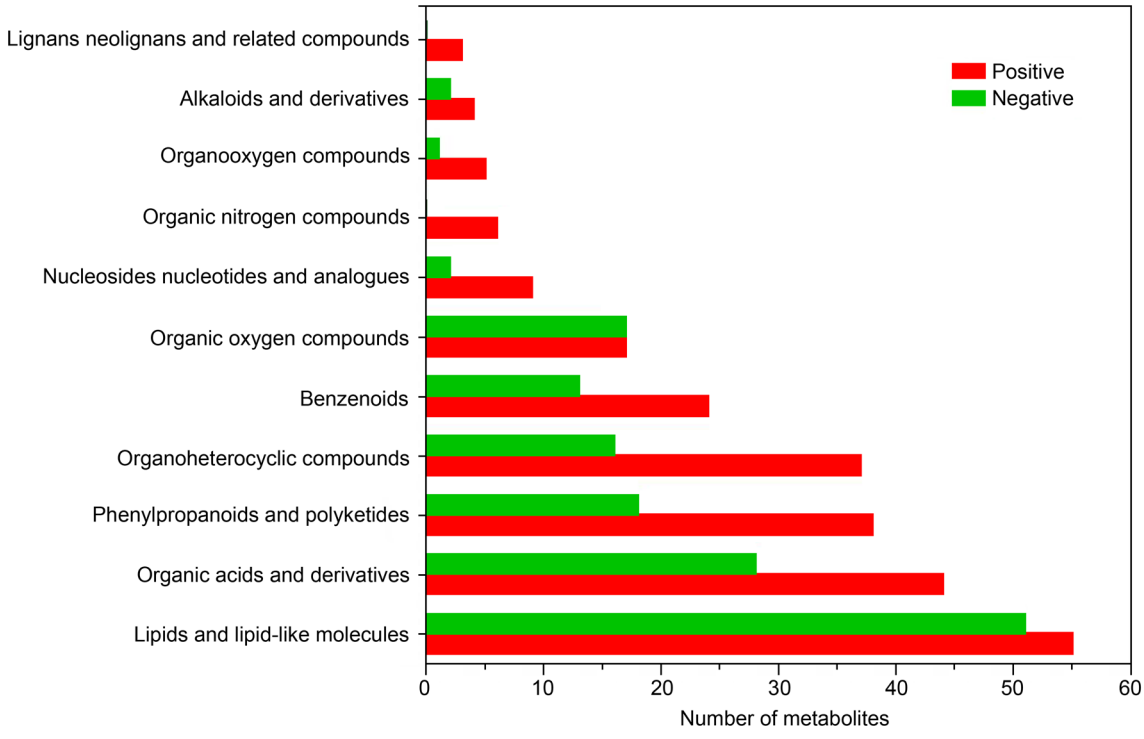

Fig. 5. HMDB classification annotation of the components of aqueous extracts of *Melia azedarach* fruits in both positive and negative ion modes. The x-axis represents metabolite numbers, and the y-axis represents annotated HMDB entries.

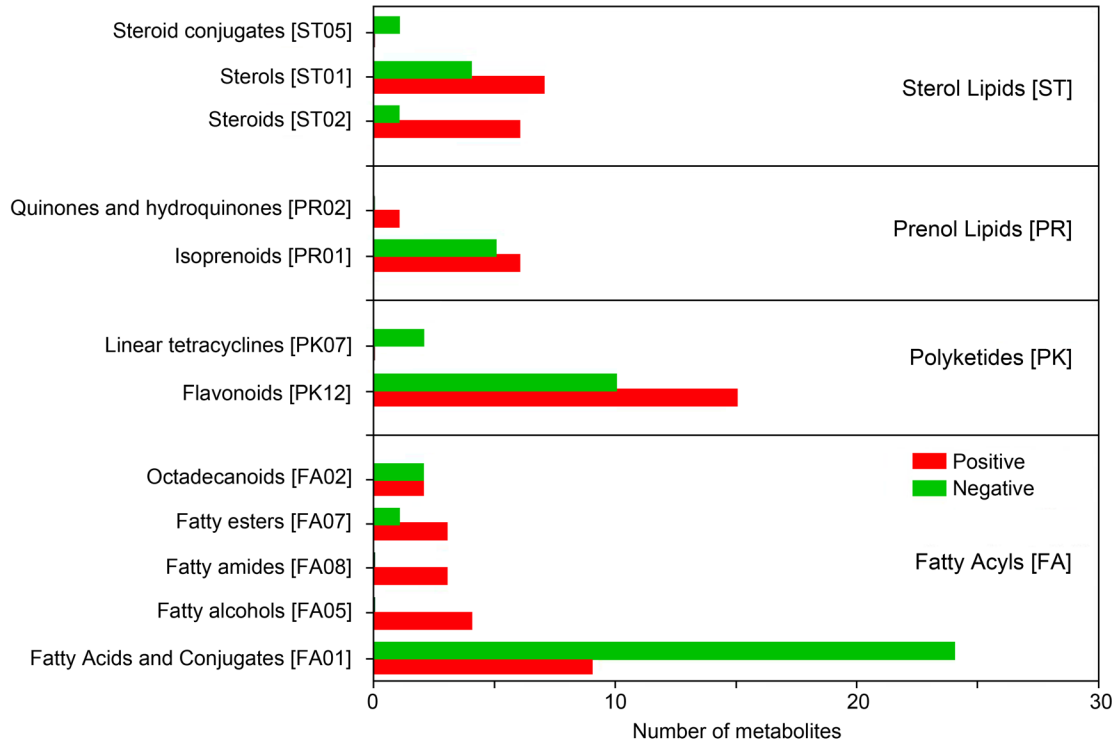

Fig. 6. Lipidmaps classification annotation of components of aqueous extracts of *Melia azedarach* fruits in both positive and negative ion modes. The x-axis represents metabolite numbers, and the y-axis represents annotated Lipidmaps entries.

comparatively lower efficiencies than those extracted by ethanol based on the agar well diffusion method or the minimum inhibitory concentrations. In addition, the petrol, benzene, ethyl acetate, methanol, and aqueous extractions of the mature seeds of chinaberry demonstrated inhibitory activities on *S. aureus* growth depending on the concentrations of the extracts, and it was also found that the most effective crude extract was

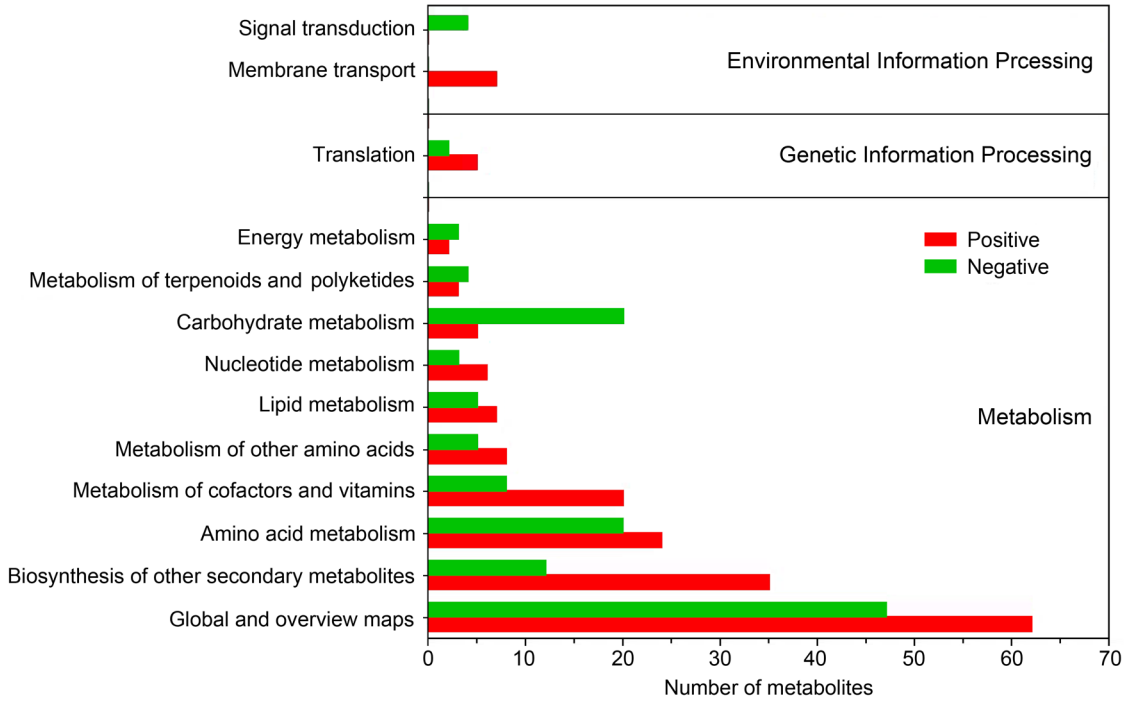

Fig. 7. KEGG enrichment chart of the components of aqueous extraction of *Melia azedarach* fruits in both positive and negative ion modes. The x-axis represents metabolite numbers, and the y-axis represents enriched KEGG pathways. KEGG, Kyoto Encyclopedia of Genes and Genomes.

not aqueous but ethyl acetate (Khan et al. 2011). The above findings, including ours, suggest that the anti-*S. aureus* efficiencies of extracts vary with the extracted parts of chinaberry. In other words, different parts of chinaberry may possess different bioactive agents that inhibit *S. aureus*.

Furthermore, *S. aureus* biofilms are cellular communities encased by self-produced three-dimensional polymers of hydrated extracellular polymeric substances (EPS) consisting primarily of water, polysaccharides, nucleic acids, proteins, and lipids (Flemming and Wingender 2010). It has been proven that biofilm-associated *S. aureus* is the pathogen of many human diseases, including osteomyelitis, endocarditis, and other infections (Götz 2002). Moreover, the construction of *S. aureus* biofilms increases its resistance to antimicrobial agents and poses a severe burden in healthcare settings (Suresh et al. 2019). Many studies have primarily focused on exploiting novel therapeutic strategies or approaches to eradicate infections associated with *S. aureus* biofilms (Lister and Horswill 2014; Bhattacharya et al. 2015; Abreu et al. 2016). In this study, we found that planktonic cells and the biofilms of *S. aureus* could be inhibited by aqueous extracts of chinaberry fruits (Fig. 1A and 2), which predicts a function for the aqueous extracts of these fruits to control *S. aureus* infections. Moreover, there is a consistent decrease in the trends of planktonic growth and biofilm formation of *S. aureus* in the presence of different concentrations of aqueous extracts of chinaberry fruits. Thus, we hypothesized that the decrease in *S. aureus* biofilm formation in the presence of aqueous extracts of chinaberry fruits might be induced by the decreases in planktonic growth (Fig. 1).

Subsequently, we sought to determine how the aqueous extracts of chinaberry fruits inhibit the growth of *S. aureus*. Therefore, the transcriptome of *S. aureus* exposed to aqueous extracts of chinaberry fruits was explored using the RNA-Seq method. The results indicated that the genes of the ribosome (pae03010), peptidoglycan biosynthesis (pae00550), DNA replication (pae03030), and phenylalanine, tyrosine, and tryptophan biosynthesis (pae00400), which are crucial for *S. aureus* protein synthesis, metabolism, and survival, were primarily inhibited by the aqueous extracts of chinaberry fruits (Fig. 3 and 4), which partially explained the mode of action of these extracts on the growth of *S. aureus*.

In addition, the crude extracts from chinaberry were evaluated for their antimicrobial efficiencies. A substantial number of active components were also separated and identified from different chinaberry parts, such as leaves, bark, fruit, and seeds. A substantial number of compounds extracted by methanol were found using GC-MS in chinaberry leaves, and the results demonstrated that the extracts contained trichloromethane, 2-pyrrolidinyl-methylamine, propanedioic acid, diethyl ester, and 2-piperidimethanamine, among others

(Al-Marzoqi et al. 2015). The ethanol extracts of chinaberry leaves exhibited significant antimicrobial activity to several bacteria, including *S. aureus*. Further isolation and identification using TLC chromatograms and GC/MS demonstrated that the compound 5,6,7,8-tetrahydro-1,2,4-benzotriazine-3-amine might be responsible for the antimicrobial activity (Kathireshan et al. 2019). A GC-MS analysis of the hexane extracts of chinaberry leaves showed a highly complex profile that contained ketones, fatty acid derivatives, ethers, 1,3-dipalmitate, methyl esters, 7,8-dihydrocarpesterol, and 2-undecanol (Habib et al. 2017). The methanolic fraction of the aerial parts of chinaberry contained steroids, anthraquinones, phenolics, flavonoids, and tannins (Malar et al. 2020). The metabolites of chinaberry flowers included branched and n-hydrocarbons, fatty acids, aromatics, fatty acid methyl esters, polyisoprenoids, and fatty alcohols (Muhammad et al. 2015). Taken together, there are various compounds extracted from various parts of chinaberry with different solvents. The extracted methods and solvents also simultaneously influenced the constituents of chinaberry extracts.

Herein, we also sought to explore the bioactive agents in the aqueous extracts of chinaberry fruits extracted in this study. Using UHPLC-MS/MS analyses, we found that the aqueous extracts from chinaberry fruits contain lipids and lipid-like molecules, organic acids and derivatives, phenylpropanoids and polyketides, organoheterocyclic compounds, and benzenoids (Fig. 5), which play an important role in inhibiting planktonic growth and biofilm formation (Fig. 1 and 2). In particular, the water extractions of chinaberry fruits also contained a substantial proportion of toosendanin, which is a potential treatment for parasites in the digestive tract and agricultural insecticides (Shi and Li 2007). It also exhibited significant inhibitory effects on the growth of *S. aureus* (data not shown). In contrast, the major components extracted from chinaberry fruits with hexane were methyl palmitate (18.8%), methyl linolenate (16.1%), and methyl linoleate (9.8%) (Hadjiakhoondi et al. 2006). A sequential extraction from chinaberry fruits was performed in four steps with $scCO_2$, a $scCO_2$/ethanol mixture, ethanol, and an ethanol/water mixture. As a result, linoleic, palmitic, and myristic fatty acids were identified in the supercritical extracts; moreover, caffeic, and malic acid were found in other extracts (Bitencourt et al. 2014).

This study demonstrated that the active components from chinaberry fruits, which inhibited the planktonic growth and biofilm formations of *S. aureus*, could be extracted using water with ultrasonic and boiling methods that are environmentally friendly. The main active components in the aqueous extracts of chinaberry fruits are lipids and lipid-like molecules, organic acids and derivatives, phenylpropanoids, polyketides, organoheterocyclic compounds, and benzenoids, which affect the gene expression of protein synthesis, metabolism, and transcriptional regulation at various levels. The results obtained in this study may help clarify the mode of action of aqueous chinaberry extracts on the growth of *S. aureus* and facilitate the further development and utilization of these extracts.

Supporting information

The detailed information, including the total ion intensity of the identified metabolites in the aqueous extracts of *M. azedarach* fruits, are available in Supplementary Excel S1 (positive mode) and S2 (negative mode).

Acknowledgments

This work was funded by the opening foundation from the State Key Laboratory of Applied Microbiology Southern China, Guangdong Institute of Microbiology (No.: SKLAM003-2018), National Natural Science Foundation of China (No.: 31770091), GDAS' Project of Science and Technology Development (Nos.: 2019GDASYL-0104006 and 2017GDASCX-0102), Natural Science Foundation of Guangdong Province (No.: 2020A151501848), and Guangdong Science and Technology Program (No.: 2017B030314045).

Conflict of interest

The authors do not report any financial or personal connections with other persons or organizations, which might negatively affect the contents of this publication and/or claim authorship rights to this publication.

Literature

Abreu AC, Saavedra MJ, Simões LC, Simões M. Combinatorial approaches with selected phytochemicals to increase antibiotic efficacy against *Staphylococcus aureus* biofilms. Biofouling. 2016 Oct; 32(9):1103–1114. https://doi.org/10.1080/08927014.2016.1232402

Al-Marzoqi AH, Hameed IH, Idan SA. Analysis of bioactive chemical components of two medicinal plants (*Coriandrum sativum* and *Melia azedarach*) leaves using gas chromatography-mass spectrometry (GC-MS). Afr J Biotechnol. 2015 Oct;14(40):2812–2830. https://doi.org/10.5897/AJB2015.14956

Archer GL. *Staphylococcus aureus*: a well-armed pathogen. Clin Infect Dis. 1998 May;26(5):1179–1181. https://doi.org/10.1086/520289

Bhattacharya M, Wozniak DJ, Stoodley P, Hall-Stoodley L. Prevention and treatment of *Staphylococcus aureus* biofilms. Expert Rev Anti Infect Ther. 2015;13(12):1499–1516. https://doi.org/10.1586/14787210.2015.1100533

Bitencourt RG, Queiroga CL, Duarte GH, Eberlin MN, Kohn LK, Arns CW, Cabral FA. Sequential extraction of bioactive compounds from *Melia azedarach* L. in fixed bed extractor using CO_2, ethanol and water. J Supercrit. Fluids. 2014 Nov;95:355–363. https://doi.org/10.1016/j.supflu.2014.09.027

Flemming HC, Wingender J. The biofilm matrix. Nat Rev Microbiol. 2010 Sep;8(9):623–633. https://doi.org/10.1038/nrmicro2415

Götz F. *Staphylococcus* and biofilms. Mol Microbiol. 2002 Mar;43(6): 1367–1378. https://doi.org/10.1046/j.1365-2958.2002.02827.x

Grabowska K, Zmudzki P, Wrobel-Biedrawa D, Podolak I. Simultaneous quantification of ursolic and oleanolic acids in *Glechoma hederacea* and *Glechoma hirsuta* by UPLC/MS/MS. Planta Med. 2021 Apr;87(4):305–313. https://doi.org/10.1055/a-1345-9377

GrayMerod R, Hendrickx L, Mueller L, Xavier J, Wuertz S. Effect of nucleic acid stain Syto9 on nascent biofilm architecture of

Acinetobacter sp. BD413. Water Sci Technol. 2005 Oct;52(7):195–202. https://doi.org/10.2166/wst.2005.0201

Habib R, Mohyuddin A, Khan Z, Mahmood T. Analysis of non-polar chemical profile of *Melia azedarach* L. Sci Inquiry Rev. 2017;1(1):49–54.

Hadadi Z, Nematzadeh GA, Ghahari S. A study on the antioxidant and antimicrobial activities in the chloroformic and methanolic extracts of 6 important medicinal plants collected from North of Iran. BMC Chem. 2020 Apr;14(1):33. https://doi.org/10.1186/s13065-020-00683-5

Hadjiakhoondi A, Vatandoost H, Khanavi M, Sadeghipour Roodsari HR, Vosoughi M, Kazemi M, Abai MR. Fatty acid composition and toxicity of *Melia azedarach* L. fruits against malaria vector *Anopheles stephensi*. Iran J Pharm Sci. 2006;2(2):97–102.

Heydorn A, Nielsen AT, Hentzer M, Sternberg C, Givskov M, Ersbøll BK, Molin S. Quantification of biofilm structures by the novel computer program COMSTAT. Microbiology. 2000 Oct; 146 (10): 2395–2407. https://doi.org/10.1099/00221287-146-10-2395

Kaneria M, Baravalia Y, Vaghasiya Y, Chanda S. Determination of antibacterial and antioxidant potential of some medicinal plants from Saurashtra region, India. Indian J Pharm Sci. 2009 Jul;71(4): 406–412. https://doi.org/10.4103/0250-474X.57289

Kathireshan AK, Priya T, Jasmine KD, Gayathri G, Kumar MRR. Assessment of *in vitro* antibacterial and antifungal activities of leaf extracts of *Melia azedarach* Linn. Indian J Pharm Sci. 2019;81(2): 380–384. https://doi.org/10.36468/pharmaceutical-sciences.520

Khalid M, Hassani D, Bilal M, Butt ZA, Hamayun M, Ahmad A, Huang D, Hussain A. Identification of oral cavity biofilm forming bacteria and determination of their growth inhibition by *Acacia arabica*, *Tamarix aphylla* L. and *Melia azedarach* L. medicinal plants. Arch Oral Biol. 2017 Sep;81:175–185. https://doi.org/10.1016/j.archoralbio.2017.05.011

Khan AV, Ahmed QU, Mir MR, Shukla I, Khan AA. Antibacterial efficacy of the seed extracts of *Melia azedarach* against some hospital isolated human pathogenic bacterial strains. Asian Pac J Trop Biomed. 2011 Dec;1(6):452–455. https://doi.org/10.1016/s2221-1691(11)60099-3

Khan MR, Kihara M, Omoloso AD. Antimicrobial activity of *Horsfieldia helwigii* and *Melia azedarach*. Fitoterapia. 2001 May;72(4): 423–427. https://doi.org/10.1016/s0367-326x(00)00334-8

Kharkwal GC, Pande C, Tewari G, Panwar A, Pande V. Volatile terpenoid composition and antimicrobial activity of flowers of *Melia azedarach* Linn. from north west Himalayas, India. J Indian Chem Soc. 2015 Jan;92(1):141–145.

Lister JL, Horswill AR. *Staphylococcus aureus* biofilms: recent developments in biofilm dispersal. Front Cell Infect Microbiol. 2014 Dec;4:178. https://doi.org/10.3389/fcimb.2014.00178

Liu S, Zeng M, Li X, Liang Y, Lei P. [Antibacterial activity of the essential oil from *Melia azedarach* flowers and chemical components analysis by GC-MS combined with chemometrics resolution method] (in Chinese). Chinese Pharm J. 2010 Oct;45(19):1508–1512.

Liu Y, Kong Z, Liu J, Zhang P, Wang Q, Huan X, Li L, Qin P. Non-targeted metabolomics of quinoa seed filling period based on liquid chromatography-mass spectrometry. Food Res Int. 2020 Nov;137:109743. https://doi.org/10.1016/j.foodres.2020.109743

Mah T-F. Biofilm-specific antibiotic resistance. Future Microbiol. 2012 Sep;7(9):1061–1072. https://doi.org/10.2217/fmb.12.76

Malar T, Antonyswamy J, Vijayaraghavan P, Kim YO, Al--Ghamdi AA, Elshikh MS, Hatamleh AA, Al-Dosary MA, Na SW, Kim HJ. *In vitro* phytochemical and pharmacological bio-efficacy studies on *Azadirachta indica* A. Juss and *Melia azedarach* Linn for anticancer activity. Saudi J Biol Sci. 2020 Feb;27(2):682–688. https://doi.org/10.1016/j.sjbs.2019.11.024

Muhammad MT, Fayyaz N, Tauseef S, Razaq U, Versiani MA, Ahmad A, Faizi S, Rasheed M. Antibacterial activity of flower of *Melia azedarach* Linn. and identification of its metabolites. J Korean Soc Appl Biol Chem. 2015 Apr;58(2):219–227. https://doi.org/10.1007/s13765-015-0029-7

Rojas Sierra JN, Pérez Cordero AF, Martínez Avilez JG, Mieles Galindo JU. [Antibacterial activity of leaf extract *Melia azedarach* L.] (in Spanish). Rev Colomb Biotecnol. 2012 Jan;14(1):224–232.

Saleem R, Ahmed SI, Shamim SM, Faizi S, Siddiqui BS. Antibacterial effect of *Melia azedarach* flowers on rabbits. Phytother Res. 2002 Dec;16(8):762–764. https://doi.org/10.1002/ptr.1044

Sen A, Batra A. Evaluation of antimicrobial activity of different solvent extracts of medicinal plant: *Melia azedarach* L. Int J Curr Pharm Res. 2012;4(2):67–73.

Shi Y-L, Li M-F. Biological effects of toosendanin, a triterpenoid extracted from Chinese traditional medicine. Prog Neurobiol. 2007 May;82(1):1–10. https://doi.org/10.1016/j.pneurobio.2007.02.002

Shukla SK, Rao TS. Effect of calcium on *Staphylococcus aureus* biofilm architecture: A confocal laser scanning microscopic study. Colloids Surf B Biointerfaces. 2013 Mar;103:448–454. https://doi.org/10.1016/j.colsurfb.2012.11.003

Stepanović S, Vuković D, Dakić I, Savić B, Švabić-Vlahović M. A modified microtiter-plate test for quantification of staphylococcal biofilm formation J Microbiol Methods. 2000 Apr;40(2):175–179. https://doi.org/10.1016/S0167-7012(00)00122-6

Suresh K, Deepa P, Harisaranraj R, Vaira Achudhan V. Antimicrobial and phytochemical investigation of the leaves of *Carica papaya* L., *Cynodon dactylon* (L.) Pers., *Euphorbia hirta* L., *Melia azedarach* L. and *Psidium guajava* L. Ethnobot Leafl. 2008 Dec;12:1184–1191.

Suresh MK, Biswas R, Biswas L. An update on recent developments in the prevention and treatment of *Staphylococcus aureus* biofilms. Int J Med Microbiol. 2019 Jan;309(1):1–12. https://doi.org/10.1016/j.ijmm.2018.11.002

Tang Q, Feng M. DPS data processing system: experimental design, statistical analysis and data mining. Beijing (People's Republic of China): Science Press; 2007.

Wright Muelas M, Roberts I, Mughal F, O'Hagan S, Day PJ, Kell DB. An untargeted metabolomics strategy to measure differences in metabolite uptake and excretion by mammalian cell lines. Metabolomics. 2020 Oct;16(10):107. https://doi.org/10.1007/s11306-020-01725-8

Zahoor M, Ahmed M, Naz S, Ayaz M. Cytotoxic, antibacterial and antioxidant activities of extracts of the bark of *Melia azedarach* (China Berry). Nat Prod Res. 2015;29(12):1170–1172. https://doi.org/10.1080/14786419.2014.982649

Zhou G, Li L, Shi Q, Ouyang Y, Chen Y, Hu W. Effects of nutritional and environmental conditions on planktonic growth and biofilm formation for *Citrobacter werkmanii* BF-6. J Microbiol Biotechnol. 2013 Dec;23(12):1673–1682. https://doi.org/10.4014/jmb1307.07041

Zhou G, Peng H, Wang Y-s, Huang X-m, Xie X-b, Shi Q-s. Enhanced synergistic effects of xylitol and isothiazolones for inhibition of initial biofilm formation by *Pseudomonas aeruginosa* ATCC 9027 and *Staphylococcus aureus* ATCC 6538. J Oral Sci. 2019; 61(2): 255–263. https://doi.org/10.2334/josnusd.18-0102

Zhou G, Shi Q, Huang X, Xie X. The three bacterial lines of defense against antimicrobial agents. Int J Mol Sci. 2015 Sep;16(9): 21711–21733. https://doi.org/10.3390/ijms160921711

Zulqarnain, Rahim A, Ahmad K, Ullah F, Ullah H, Nishan U. *In vitro* antibacterial activity of selected medicinal plants from lower Himalayas. Pak J Pharm Sci. 2015 Mar;28(2):581–587.

Supplementary materials are available on the journal's website.